Experimental Investigation of Developing Spray Boiling on a Flat Flake Surface with Constant Heat Flux

Zhongyuan Shi and Tao Dong

1 Introduction

Spray evaporation cooling is to deliver liquid droplet, of which the diameter is usually stated in micrometers, to the heated surface where the boiling droplets works as heat sink with significantly high heat flux, to which the field synergy [1] of spray droplet velocity and temperature gradient is believed to contribute. This technology has been widely utilized in many applications, e.g. metallurgy, machining, chemical industry, aerospace engineering, nuclear power plant safety, etc.

Konpchikov [2] is among the first authors who conducted experiments on spray cooling. It was reported that the critical heat flux is more than four times of that from pool boiling (up to 500 W/cm^2 with a superheat of 20°C), pressurized water atomized when leaving the nozzle outlet, of which the diameter is 0.02-0.2mm. Toda [3][4] proposed a curve of wall superheat vs. heat flux by fitting the experimental data. It was claimed that the spray droplets with a mean diameter of 117μm (estimated) and a mean velocity of 72.4m/s (estimated) impinged onto a circular wall surface of which the diameter and superheat are 15mm and 50°C respectively, yielding a heat flux of 400W/cm^2. The critical heat flux rises with the increasing subcooled temperature, spray mass flow rate and droplet velocity individually. Bonacinna [5] investigated the spray cooling characteristics under low flow rate distribution density and low excess temperature. When the superheat is 35°C and only 19% of the heated surface is covered by spray droplets, the heat flux is 215W/cm^2. In the experiment, the droplet diameter is reported as 89.5μm with a velocity of 2m/s. Also, the droplets tend not to rebound when its impacting velocity is low. Monde [6] analyzed the effect of spray flow rate and droplet velocity. Bubbles get formed on the heated surface with splashing droplets while the heat flux increases with spray flow rate. Tilton and Pais [7] claimed a much higher critical heat flux of 1100W/cm^2 compared to all the previously reported values when the superheat is 60°C, laser granulometry applied in the investigation. Yao and Choi [8] reported that the heat flux increases with spray mass flow rate with a droplet velocity range of 2.72-5.84m/s and a droplet diameter range of 0.407-0.530mm. According to their experimental result, ,the effect of impacting velocity of droplets on heat transfer is not significant within the film boiling region whereas in the nucleate and the transitional boiling region, the impact of impinging velocity is considerable. Using the same spray system and test piece, Choi and Yao [9] further explored the effect of spray direction on heat transfer characteristics. In the film boiling region, vertical spray (VS) yielded obviously higher heat transfer coefficient than that from horizontal spray (HS), which is caused by the secondary impact of the rebounded droplets. However, in the transitional boiling region, HS resulted in higher heat transfer coefficient, which is probably due to the fact that it is easier for bubbles to get detached from the test piece surface with HS. Yang [10] used gas-liquid mixing nozzle in the experimental study. The heat transfer coefficient was found increasing with spray flow rate. Increasing gas velocity within the nozzle enhances the heat transfer by generating droplets of smaller size and thinner boundary layer.

In boiling regions, surface condition is one of the important factors to the distribution and number of boiling nuclei. It is believed that rough surface facilitates the generation of boiling nuclei and therefore the heat transfer [11]. On the other hand, surfaces that cannot get wetted easily is also believed to be helpful to the formation of boiling nuclei, which led to higher heat flux when the wall temperature is between 100°C and the temperature corresponding to critical heat flux [12]. Nevertheless, no consensus has been reached toward the effect of surface roughness. Sehmbey [12]

Z. Shi • T. Dong (✉)
Norwegian Center of Expertise on Micro- and Nano Technologies, Department of Micro and Nano Systems Technology (IMST), Faculty of Technology and Maritime Sciences (TekMar), Buskerud and Vestfold University College (HBV), Borre N-3199, Norway
e-mail: Zhongyuan.Shi@hbv.no; Tao.Dong@hbv.no

H. Selvaraj et al. (eds.), *Progress in Systems Engineering: Proceedings of the Twenty-Third International Conference on Systems Engineering*, Advances in Intelligent Systems and Computing 1089,
DOI 10.1007/978-3-319-08422-0_16, © Springer International Publishing Switzerland 2015

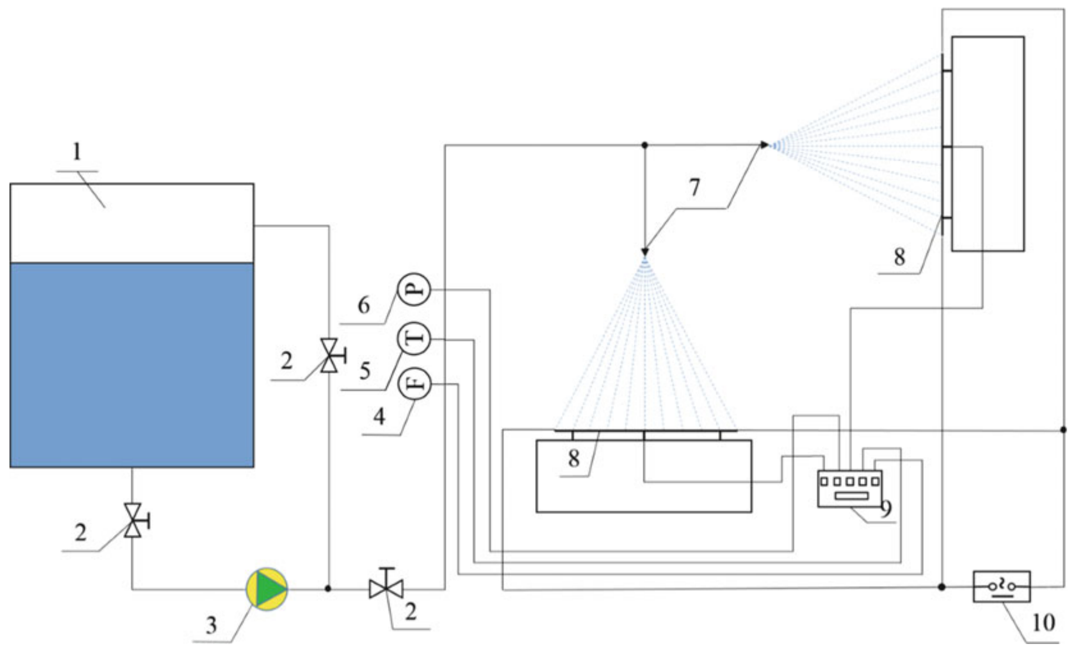

Fig. 1 Schematic representation of experiment system with 1 – water tank, 2 – needle valve, 3 – centrifugal pump, 4 – turbine flowmeter, 5 – platinum resistance thermometer, 6 – pressure gauge, 7. solid cone spray nozzle, 8. test piece – a stainless steel flake, 9 – multimeter, 10 – electric power supply

reported an apparent enhancement on heat transfer coefficient for smoother surfaces (averaged roughness less than 0.1μm) with gas-liquid mixing nozzle. But for normal pressure nozzle, rougher surfaces resulted in higher heat flux. Bernardin [13] also found that rougher surfaces intensifies the heat transfer in nucleate boiling and part of the transitional boiling region.

Most of the relevant work are presented concerning established boiling regions, i.e. nucleate boiling, transitional boiling and film boiling whereas cases for subcooled or developing nucleate boiling are rarely seen in published literature. In the present work, the effect of such premature boiling will be investigated in regard of both horizontal and vertical spray droplets impacting on a flat flake with constant heat fluxes. A new data reduction method will be proposed for a more reasonable interpretation of the heat transfer performance variation in this region.

2 Test Setup

Fig. 1 shows the test setup mainly consisting of the piping system, the electric power for heating the test piece, the data acquisition set and the support frame with the distance from nozzle exit to the test piece surface (nozzle-to-surface distance, L) adjustable. The connecting line between the nozzle exit and the geometric centroid of the test piece is normal to the droplet-impacted surface plane of the test piece. The spray fluid, i.e. water in the present study, is delivered to the nozzle by a centrifugal pump with high head and low flow rate. For the spray flow rate (V) to be tuned more precisely, two needle valves are installed in the system, one on the bypass pipeline at the outlet of the pump, the other on the main branch leading to the nozzle.

The adjustable electric power is connected to the brass poles fixed at two ends of the test piece (170mm× 20mm×0.05mm, stainless flake), together with the gel layer for thermal insulation on the back side of the test piece to ensure the controllable heat generation within the test piece is removed by impacting droplets.

Since the spray flow rate is not always uniformly distributed within the cross sectional plane of the spray jet [14], two thermocouples are fixed on the back side of the test piece, aligned with the longitude center axis and circular-symmetric to the geometric centroid where a third thermocouple is fixed. The spray temperature, pressure (p) and flow rate are acquired respectively from the platinum resistance thermometer, pressure gauge and the turbine flow meter before the nozzle.

Before the experimental tests, the supply water temperature in the water tank was adjusted to an appropriate value. To evacuate the stagnant air in the piping system, the pump was working with relatively higher speed for a period of time. Spray mass flow rate was adjusted to a desired value before the test piece got heated by input electric power. To ensure the accuracy, each datum point was obtained by

Fig. 2 Local details of test piece with temperature measurement

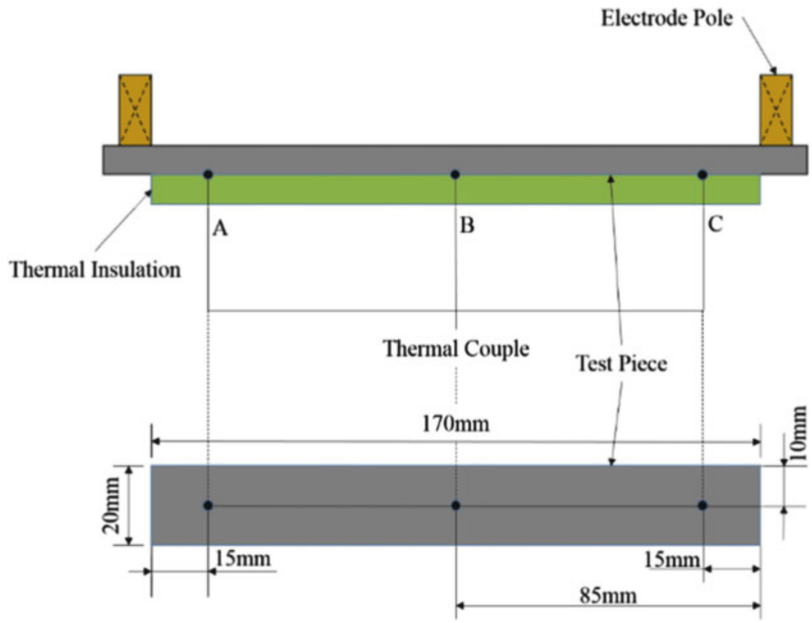

averaging auto-acquisition scans at steady-state. The multimeter was connected to a computer program for data logging and reduction which is discussed below.

3 Data Reduction

As aforementioned the test piece heated by the input electric power will be regarded as a heat source with constant wall flux [15] which yields

$$q = \frac{Q}{A} \tag{1}$$

in which Q (W) – total power input to the test piece, A (m^2) –area of the test piece surface, q (W/m^2) – wall heat flux on the test piece surface, note that test piece surface hereinafter refers to that in direct contact with incoming droplets.

The heat transfer coefficient is thereafter obtained by,

$$\begin{cases} h_{sp} = \dfrac{q}{T_w - T_f}, \; for \; T_w \le T_s \\ h_b = \dfrac{q}{T_w - T_s}, \; for \; T_w \ge T_s \end{cases} \tag{2}$$

where h_{sp} (W/m^{2}K) and h_b (W/m^{2}K) represent the heat transfer coefficient for single phase impinging convection (SPIC) and boiling while T_w, T_f and T_s are for temperature of the test piece surface, spray fluid temperature and saturation temperature corresponding to the ambient pressure in which spray impinging evaporation takes place, respectively.

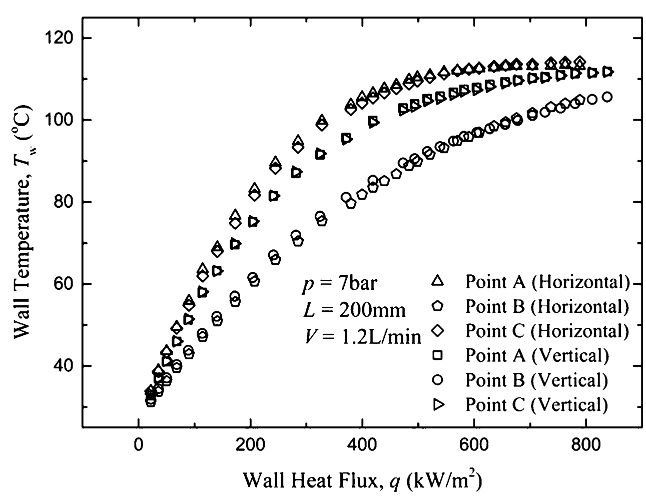

Fig. 3 Variation of wall heat flux with temperature at different locations

4 Result and Discussion

Fig. 3 shows the performance of spray cooling with a volumetric flow rate of 1.2L/min and a nozzle-to-surface distance of 200mm. The temperature at Point B is the lowest compared by those from Point A and C, which overlap with each other, given the same wall heat flux. It is therefore presumably inferred that the local mass flux is larger at the location near to the spray jet axis (SJA) and decreases symmetrically in the radial direction perpendicular to SJA.

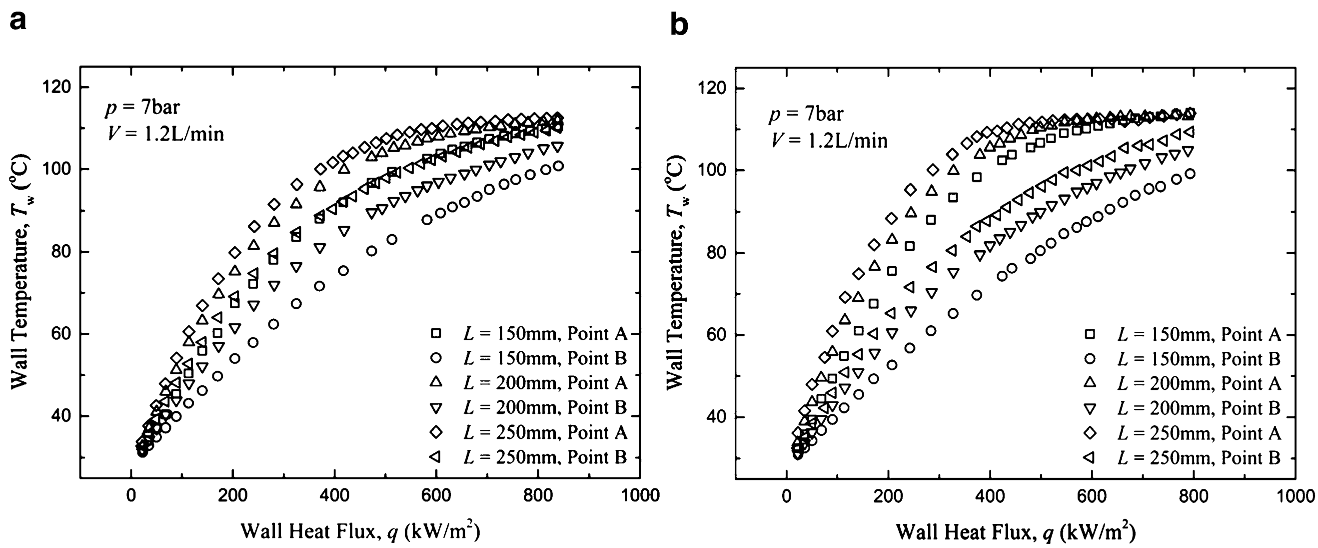

Fig. 4 Variation of wall heat flux with temperature under different nozzle-to-surface distances for (**a**) VS cases and (**b**) HS cases

The slope of wall temperature starts to decrease significantly with rising heat flux in a wall temperature region near to the saturation point, i.e. 100°C in the present study especially for locations (Point A and C) with less impinging mass flux, whereas for the near-to-SJA region (Point B) the slop decreases more smoothly and tends to continue decreasing even after the counterpart at Point A or C stalls (temperature reaching a constant value). This is probably because of the trade-off between two major mechanisms dominating heat transfer, the SPIC and the boiling. When the local spray flux is low, the effect of SPIC gets dominated by that of boiling more "quickly" with the increasing wall heat flux.

Compared to cases for HS, the VS cases yielded higher heat flux at Point A and C where the local spray mass flux is lower, indicating a possible enhancement from rebounded droplet [9]. For Point B, no obvious difference is observed between the VS and the HS cases. On the other hand, a smoother slope decreasing can be identified for all the VS cases (Point B included), again the effect of SPIC is supposedly retarding the transition to boiling dominated regime.

Fig. 4(b) shows the effect of spray distance on spray cooling performance. Since the temperature profile at Point A simply overlap with that at Point C (like in Fig. 4(a)), only one of these two profiles will be involved in the following discussion (see Fig. 4(b)) to avoid confusion. For a certain location under measurement, either point A or B, the local surface temperature (LST) increases with increasing nozzle-to-surface distance whereas the increasing magnitude (IM) is not uniform. Before the temperature measured at a certain point reaches the saturation temperature, the IM increases with increasing heat flux at different nozzle-to-surface distances. When LST goes beyond the saturation temperature, the IM decreases with increasing heat flux. This trend is more obvious in the location (Point A) with less impinging mass flux [18], which is reasonable compared to the location (Point B) where the retarding effect of SPIC is significant and the IM decreases slower.

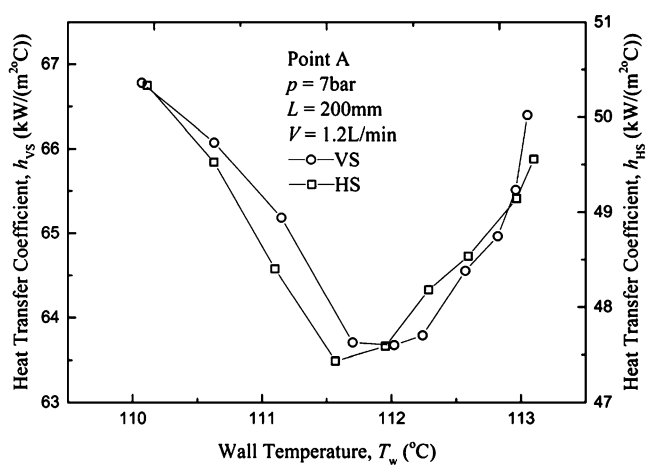

Fig. 5 Variation of heat transfer coefficient with wall temperature in the boiling region

A similar trend is observed for the HS cases in Fig. 4(b). Nevertheless, the effect of SPIC is more dominating in horizontal cases since the temperature difference between locations with different impinging mass flux is larger compared to that of the VS cases given all other conditions unchanged.

The heat transfer coefficient in the boiling region, h_b calculated by Eq. (2) with $T_w > 110$°C is shown in Fig. 5. A decreasing-increasing trend with a local minimum (at

T_w = 111.6°C and 112°C for HS and VS respectively) is observed for h_b with increasing T_w. However, according to the conventional boiling heat transfer theory, it is expected that the heat transfer keeps getting intensified with an increasing wall heat flux before the critical heat flux is reached, which indicates that the conventional data reduction method for heat transfer coefficient in Eq. 2 may need modification.

The existing report [16][17] on subcooled pool boiling involves two major characteristic turning points. One is the onset of nucleate boiling(ONB) corresponding to a wall temperature of T_{ONB} below which heat transfer is principally determined by single phase convection. Bubbles start to form on and get attached to the wall surface when the wall temperature keeps rising to T_{ONB} and beyond, accompanied by a substantial increase in wall heat flux and heat transfer coefficient. The other is the onset of fully developed boiling (OFDB) marked by a wall temperature of T_{OFDB} beyond which bubbles get detached from the heated wall surface. The concept can be analogously adopted for spray impinging evaporation.

The wall heat flux is comprised of two components induced by SPIC (q_{SPIC}) and nucleate boiling (q_{nb}) individually [18] where

$$q_{SPIC} = h_0 (T_w - T_f) \left(\frac{\mu_f}{\mu_w} \right)^n \tag{3}$$

where h_0 and n are constants from regression, μ_f and μ_w are dynamic viscosity of water based on the spray fluid temperature and the wall temperature respectively and

$$q_{nb} = q - q_{SPIC}. \tag{4}$$

Following Eq. (3) and Eq. (4), the SPIC and the nucleate boiling heat transfer coefficient are redefined as

$$h_{SPIC} = h_0 \left(\frac{\mu_f}{\mu_w} \right)^n \tag{5}$$

and

$$h_{nb} = \frac{q_{nb}}{(T_w - T_s)} \tag{6}$$

respectively.

Fig. 6 shows the comparison of the experimental wall heat flux and the calculated SPIC wall heat flux. For both HS and VS cases, the experimental heat flux the deviates from the calculated value to a considerably higher magnitude starting from approximately T_w=100°C, which resembles the ONB in pool boiling. Back to Fig. 5, heat transfer coefficient decreases before the local minimum, which is probably caused by the fact that attached bubbles are limiting the space for single phase convection in the near-to-wall region within the liquid film layer on the heated surface. T_w increasing after the local minimum, the heat transfer coefficient begins to increase which is probably due to the enhanced single phase convection by the "stirring" effect of bubbles' motion leaving the heated surface [16] which rationalizes marking the local minimum as OFDB.

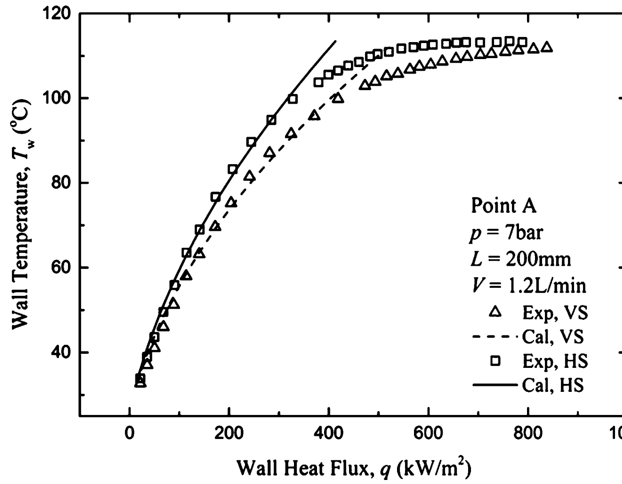

Fig. 6 Boiling curve, experimental vs. calculated from regression

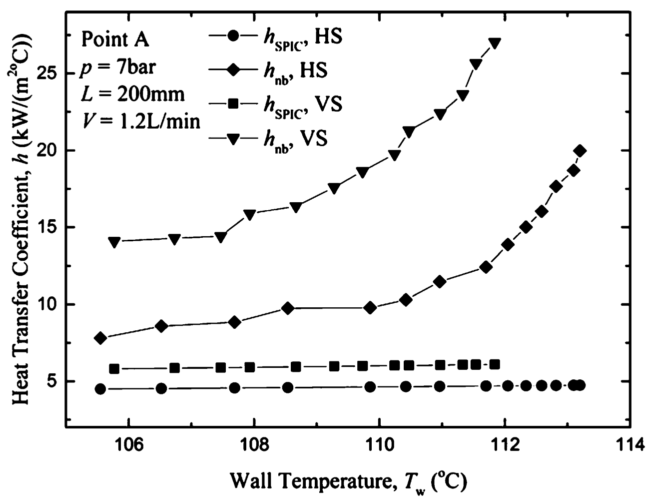

Fig. 7 Heat transfer performance in transition to fully developed boiling

As shown in Fig. 7, the nucleate boiling component of the heat transfer coefficient h_{nb} increases monotonically with increasing T_w, which avoids the anomalously posed trend in Fig. 5. On the other hand, the SPIC component also increases with ascending T_w but a negligible slope compared to its counterpart.

When the wall heat flux reached a certain value in correspondence with that greater than the rightmost wall temperatures for HS or VS cases individually, the test piece would be burnt into two parts from the region close to the centerline normal to the longitude direction, which is similar to the critical point of pool boiling that droplets evaporated almost immediately after contacting the heated surface before the next batch of droplets arrives so that any effort to achieve a higher wall heat flux will result in a growth spurt of temperature and burn the test piece apart.

However, the difference is for pool boiling, the heated surface usually get burnt after a significant heat transfer coefficient decrease which is not observed in the present investigation, which might be caused by the fact that the thin steel flake get burnt too fast (within the minimum increasing step of power input to the test piece) before any data could be collected.

5 Conclusion

In the present study, the heat transfer performance of water spray impinging on a heated steel flake is investigated with respect to the effect of spray direction, nozzle-to-surface distance and wall heat flux. The VS cases yield higher heat transfer coefficient than that of the HS cases. The nozzle-to-surface distance has influence on the local impinging mass flux, which affects the heat transfer coefficient considerably. The heat transfer performance is dominated by SPIC and nucleate boiling sequentially with increasing wall heal flux.

Conventional data reduction method yields an irrational heat transfer variation with increasing wall temperature when the enhancement mechanism is moving forward to the fully developed boiling region in analogy to pool boiling. The proposed decomposition of wall heat flux separates the nucleate boiling heat transfer coefficient from the conventional all-in-one heat transfer coefficient based on which a physically more credible variation trend is achieved.

Acknowledgment The present work is primarily supported by Forskningsradet Nærings-Ph.d (Project No.: 231952), Scientific Research Project (Project No. A2620110012), VRI bedriftsmidler (Project No.: 235042) and Regionale Forskningsfond Oslofjordfondet (Project No.: 235809). The Research Council of Norway is acknowledged for the support through the Norwegian Micro- and Nano-Fabrication Facility, NorFab (197411/V30). The RotoBoost AS which initiates and facilitates the present work is hereby acknowledged.

References

1. Guo, Z. Y., Tao, W. Q., Shah, R. K.: The Field Synergy (Coordination) Principle and its Applications in Enhancing Single Phase Convective Heat Transfer. Int J Heat Mass Transfer 48(9), 1797–1807 (2005)
2. Kopchikov, I. A., Voronin, G. I., Kolach, T. A., Labuntsov, D. A., Lebedev, P. D.: Liquid Boiling in a Thin Film. Int. J. Heat Mass Transfer 12(7), 791–796 (1969)
3. Toda, S.: A Study of Mist Cooling : 1st Report, Experimental Investigations on Mist Cooling by Mist Flow Sprayed Vertically on Small and Flat Plates Heated at High Temperatures. Trans. JSME 38(307), 581–588 (1972)
4. Toda, S.: A Study of Mist Cooling (2nd Report : Theory of Mist Cooling and its Fundamental Experiments). Heat Transfer Japanese Research 3, 1–44 (1974)
5. Bonacina, C., Comini, G., Del Giudice, S.: Dropwise Evaporation. J. Heat Transfer 101(3), 441–446 (1979)
6. Monde, M., Inoue, T.: Critical Heat Flux in Saturated Forced Convective Boiling on a Heated Disk With Multiple Impinging Jets. J. Heat Transfer 113(3), 722–727 (Aug 1991)
7. Pais, M., Tilton, D., Chow, L., Mahefkey, E.: High-Heat-Flux, Low-Superheat Evaporative Spray Cooling. In : 27th Aerospace Sciences Meeting (January 1989)
8. Yao, S. C., Choit, K. J.: Heat Transfer Experiments of Mono-Dispersed Vertically Impacting Sprays. Int. J. Multiphase Flow 13 (5), 639–648 (1987)
9. Choi, K. J., Yao, S. C.: Mechanisms of Film Boiling Heat Transfer of Normally Impacting Spray. Int J Heat Mass Transfer 30(2), 311–318 (1987)
10. Yang, J. D., Pais, M. R., Chow, L. C.: High Heat Flux Spray Cooling. In : Proc. SPIE 1739, High Heat Flux Engineering (1993)
11. Rohsenow, W. M., Hartnett, J. P., Cho, Y. I.: Handbook of Heat Transfer 3rd edn. McGraw-Hill, New York (1998)
12. Sehmbey, S. M., Pais, R. M., Chow, C. L.: Effect of surface material properties and surface characteristics in evaporative spray cooling. In : 5th Joint Thermophysics and Heat Transfer Conference, AIAA and ASME, Seattle, pp.505–512 (1990)
13. Bernardin, J. D., Stebbins, C. J., Mudawar, I.: Effects of Surface Roughness on Water Droplet Impact History and Heat Transfer Regimes. Int J Heat Mass Transfer 40(1), 73–88 (1996)
14. Yuan, W. X., Liu, C. X., Zhao, X. S., Zeng, T.: Development and Application of System for Measurement on the Spray Cooling Feature of Nozzle (in Chinese). Steelmaking 20(1), 36–39 (May 2004)
15. Lei, S. Y.: Investigation on Spray Cooling Mechanism and Nonboiling Model (in Chinese). (2002) National Natural Science Foundation of China (No. 50176025).
16. Bergman, T. L., Lavine, A. S., Incropera, F. P., DeWitt, D. P.: Fundamentals of Heat and Mass Transfer 7th edn. Wiley, Hoboken, USA (2011)
17. Maprelian, E., Castro, A. A. d., Ting, D. K. S.: Onset of Nucleate Boiling and Onset of Fully Developed Subcooled Boiling Detection Using Pressure Transducers Signals Spectral Analysis. In : 15th Brazilian Congress of Mechanical Engineering, São Paulo, Brazil (1999)
18. Chen, W. K.: Research on Efficient Spray Impinging Evaporation Heat Transfer Technology under Small Temperature Differences (in Chinese). Master Thesis, University of Shanghai for Science and Technology, Shanghai (2007)